The EMBO Journal Vol.17 No.20 pp.5896–5904, 1998

Crystal structure of an angiogenesis inhibitor bound to the FGF receptor tyrosine kinase domain

Moosa Mohammadi[1], Scott Froum[2], James M.Hamby[3], Mel C.Schroeder[3], Robert L.Panek[4], Gina H.Lu[4], Anna V.Eliseenkova[1], David Green[2], Joseph Schlessinger[1,5,6] and Stevan R.Hubbard[1,5,6]

Departments of [1]Pharmacology and [2]Medicine, [2]Kaplan Comprehensive Cancer Center, and [5]Skirball Institute of Biomolecular Medicine, New York University Medical Center, New York, NY 10016 and Departments of [3]Chemistry and [4]Therapeutics, Parke-Davis Pharmaceutical Research, Division of Warner-Lambert Company, Ann Arbor, MI 48105, USA

[6]Corresponding authors
e-mail: hubbard@tallis.med.nyu.edu

Angiogenesis, the sprouting of new blood vessels from pre-existing ones, is an essential physiological process in development, yet also plays a major role in the progression of human diseases such as diabetic retinopathy, atherosclerosis and cancer. The effects of the most potent angiogenic factors, vascular endothelial growth factor (VEGF), angiopoietin and fibroblast growth factor (FGF) are mediated through cell surface receptors that possess intrinsic protein tyrosine kinase activity. In this report, we describe a synthetic compound of the pyrido[2,3-*d*]pyrimidine class, designated PD 173074, that selectively inhibits the tyrosine kinase activities of the FGF and VEGF receptors. We show that systemic administration of PD 173074 in mice can effectively block angiogenesis induced by either FGF or VEGF with no apparent toxicity. To elucidate the determinants of selectivity, we have determined the crystal structure of PD 173074 in complex with the tyrosine kinase domain of FGF receptor 1 at 2.5 Å resolution. A high degree of surface complementarity between PD 173074 and the hydrophobic, ATP-binding pocket of FGF receptor 1 underlies the potency and selectivity of this inhibitor. PD 173074 is thus a promising candidate for a therapeutic angiogenesis inhibitor to be used in the treatment of cancer and other diseases whose progression is dependent upon new blood vessel formation.

Keywords: angiogenesis/fibroblast growth factor/tyrosine kinase inhibitor/vascular endothelial growth factor/X-ray crystallography

Introduction

Angiogenesis is the process by which new blood vessels are formed from pre-existing vasculature. This multi-stage process is initiated by the secretion of angiogenic factors that induce capillary endothelial cells to release proteolytic enzymes. The resulting degradation of the local basement membrane allows proliferation and invasion of endothelial cells into the surrounding stroma. The endothelial cells subsequently change shape and tightly adhere to one another to form the lumen of a newly formed capillary tube (reviewed in Risau, 1997). Angiogenesis occurs during normal embryonic development and is restricted in adults to processes associated with female reproductive cycles and wound healing. Pathological angiogenesis is a feature of various disease conditions such as diabetic retinopathy, atherosclerosis and psoriasis. Moreover, it is now widely recognized that tumor growth and metastasis are dependent upon new blood vessel formation (reviewed in Hanahan and Folkman, 1996). Consequently, a considerable effort is underway to develop angiogenesis inhibitors for therapeutic use.

Angiogenesis involves the concerted action of a number of polypeptide factors such as vascular endothelial growth factor (VEGF), angiopoietin 1 (Ang1) and fibroblast growth factor (FGF) (reviewed in Folkman and D'Amore, 1996). The VEGF and FGF families of polypeptide growth factors are both mitogenic and chemotactic for endothelial cells. Ang1 is not mitogenic for endothelial cells, but rather is a positive regulator of the assembly of non-endothelial cells at newly formed vessels (Davis *et al.*, 1996; Suri *et al.*, 1996). The angiogenic properties of these polypeptide factors are mediated by cell surface receptors with intrinsic protein tyrosine kinase activity (reviewed in Ullrich and Schlessinger, 1990), of which there are three mammalian VEGF receptors: VEGFR1 (Flt-1), VEGFR2 (Flk-1/KDR) and VEGFR3 (Flt-4) (reviewed in Mustonen and Alitalo, 1995); four FGF receptors: FGFR1-4 (reviewed in Jaye *et al.*, 1992); and two TIE receptors: TIE1 (Partanen *et al.*, 1992) and the Ang1 receptor TIE2/Tek (Dumont *et al.*, 1992). There is a large body of evidence supporting the role of VEGF, Ang1 and their receptors in the formation of the vascular system (Dumont *et al.*, 1994; Fong *et al.*, 1995; Puri *et al.*, 1995; Sato *et al.*, 1995; Shalaby *et al.*, 1995; Carmeliet *et al.*, 1996). For example, Flt-1- and Flk-1-deficient mice die at early stages of embryonic development due to lack of or abnormalities in vascular structures (Fong *et al.*, 1995; Shalaby *et al.*, 1995).

Despite having potent angiogenic activity, FGFs have not been shown to be directly involved in angiogenesis during development. Nevertheless, FGFs have been clearly implicated in tumor angiogenesis. FGFs are produced by neovascularizing tumors (Libermann *et al.*, 1987), and FGF levels are known to be elevated in the serum and urine of cancer patients (Fujimoto *et al.*, 1991; Nguyen *et al.*, 1994). Moreover, injection of human melanomas with anti-sense cDNAs for basic FGF (bFGF) or FGFR1 blocked intratumoral angiogenesis, resulting in the regression of tumors and the onset of necrosis (Wang and Becker, 1997).

VEGF also plays an important role in tumor angiogenesis. Inhibition of VEGF signaling by antibodies against VEGF (Kim *et al.*, 1993) or by a dominant-negative Flk-1 mutant (Millauer *et al.*, 1994) slows tumor growth. Yet recent studies have shown that suppression of VEGF signaling had no effect on the growth of large tumors, and that other angiogenic factors such as bFGF can substitute for VEGF (Yoshiji *et al.*, 1997). Therefore, targeting only the VEGF signaling pathway for inhibition may result in the emergence of tumor cell clones that produce alternative angiogenic factors. Indeed, primary breast cancers were shown to produce up to six different polypeptides with angiogenic activity, including acidic FGF (aFGF), bFGF and VEGF (Relf *et al.*, 1997). Thus, to be clinically effective, anti-angiogenesis therapy may require blockage of more than one angiogenic pathway.

Screening of a chemical compound library for inhibitors of the FGF and platelet-derived growth factor (PDGF) receptors has led to the identification of a novel class of tyrosine kinase inhibitors based on a pyrido[2,3-*d*]pyrimidine core (Connolly *et al.*, 1997). Chemical modifications of this core yielded compounds with different selectivity profiles for protein kinases. One such compound, designated PD 173074, was found to be highly selective for the FGF receptor. We report here that in cultured cells PD 173074 is a nanomolar inhibitor of FGFR1 and is also a submicromolar inhibitor of VEGFR2. We have tested this compound for its ability to block angiogenesis *in vivo* in a mouse corneal pocket assay, and present data showing that PD 173074 is an effective inhibitor of angiogenesis induced by either FGF or VEGF, with no observed toxicity. In addition, we have determined the crystal structure of PD 173074 bound to the FGFR1 tyrosine kinase domain to understand how selectivity is achieved, with an aim towards developing new angiogenesis inhibitors with increased potency.

Results and discussion

Inhibition of kinase activity in vitro and in NIH 3T3 cells

The lead compound identified in a screen for inhibitors of the FGF and PDGF receptors contains a pyrido[2,3-*d*]pyrimidine core with an attached 2,6-dichloro phenyl group at the 6-position (Connolly *et al.*, 1997). This compound showed a relatively broad selectivity profile for tyrosine kinases, with a half-maximal inhibitory potency (IC_{50}) in the range 100 nM to 10 μM. Substitution with a 3,5-dimethoxy phenyl group at the 6-position and addition of a dialkylaminoalkyl group at the 2-position yielded a compound, PD 173074 (Figure 1A), that exhibits nanomolar potency and high selectivity for the FGF receptor. *In vitro* kinase inhibition assays were performed for several tyrosine and serine/threonine kinases. PD 173074 inhibited the kinase activity of FGFR1 *in vitro* with an IC_{50} of ~25 nM, while inhibiting Src, the receptors for insulin, epidermal growth factor (EGF) and PDGF, as well as several serine/threonine kinases with 1000-fold or greater IC_{50} values (Table I). Analysis of reaction kinetics as a function of ATP concentration revealed that PD 173074 was an ATP-competitive inhibitor of FGFR1 with an inhibitory constant (K_i) of ~40 nM.

Next we examined the ability of PD 173074 to inhibit

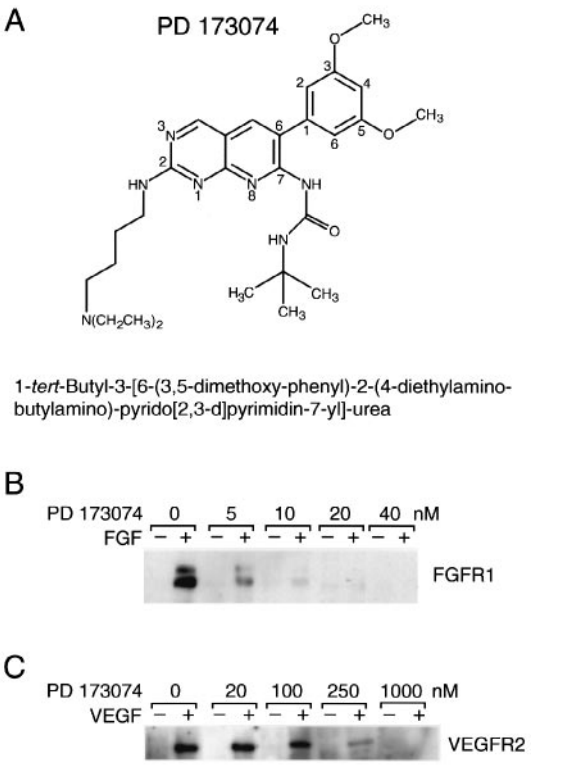

Fig. 1. Inhibition of FGFR1 and VEGFR2 autophosphorylation in NIH 3T3 cells. (**A**) Chemical structure of PD 173074. (The synthesis of PD 173074 is described in U.S. Patent 5733913). (**B**) NIH 3T3 cells were incubated with various concentrations of PD 173074 for 5 min at 37°C and then stimulated with aFGF (100 ng/ml) and heparin (10 μg/ml) (+) or left unstimulated (–) for 5 min at 37°C. Cell lysates were immunoprecipitated with antibodies to FGFR1, separated by SDS–PAGE (8%), and immunoblotted with antibodies to phosphotyrosine. Approximately equal numbers of receptors were immunoprecipitated in each case (data not shown). (**C**) NIH 3T3 cells overexpressing VEGFR2 (Flk-1) were incubated with various concentrations of PD 173074 for 5 min at 37°C and then stimulated with VEGF (100 ng/ml) (+) or left unstimulated (–) for 5 min at 37°C. Cell lysates were subjected to SDS–PAGE (8%) and immunoblotted with antibodies to phosphotyrosine.

Table I. PD 173074 inhibitory constants

Protein kinase[a]	IC_{50}[b]	K_i[c]
FGFR1	21.5 ± 0.8 nM (8)[d]	45.2 ± 4.8 nM (3)
FGFR1 (cyto.)[e]	28.9 ± 1.9 nM (6)	36.4 ± 3.6 nM (3)
PDGFR (cyto.)	17.6 ± 1.9 μM (4)	N.D.[f]
c-Src	19.8 ± 2.3 μM (4)	N.D.
EGFR	>50 μM (1)	N.D.
InsR	>50 μM (1)	N.D.
MEK	>50 μM (1)	N.D.
PKC[g]	>50 μM (1)	N.D.

[a]Abbreviations not defined in the text: InsR, insulin receptor; MEK, mitogen-activated protein kinase (MAPK) kinase; PKC, protein kinase C.
[b]Values are the mean ± standard error of the concentration of inhibitor producing 50% inhibition of kinase activity.
[c]Values are the mean ± standard error of the dissociation constant of the inhibitor–enzyme complex.
[d]The number of separate experiments performed in triplicate is given in parentheses.
[e]cyto. = cytoplasmic domain.
[f]N.D. = not determined.
[g]A mixture of α, β and γ isotypes was tested.

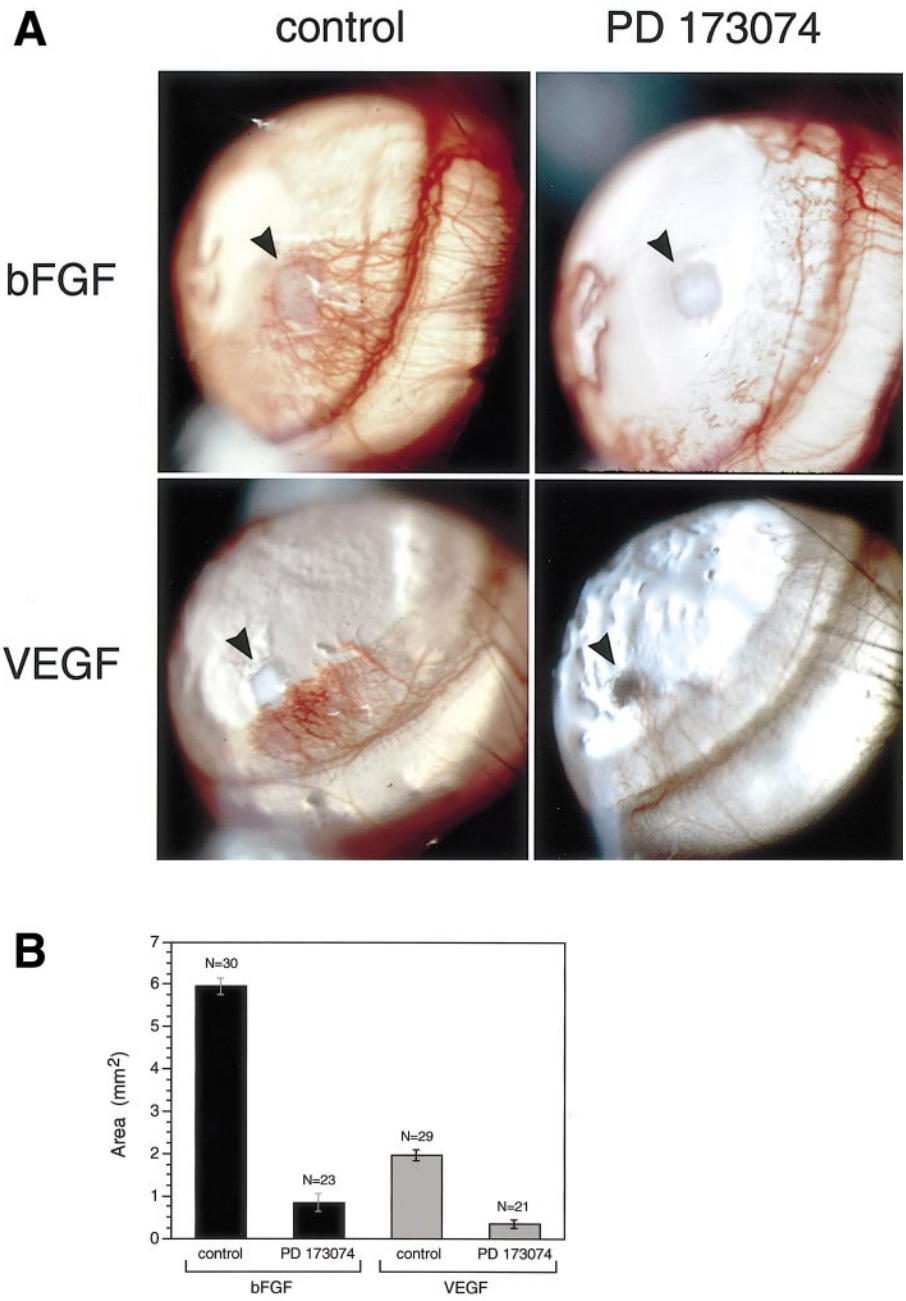

Fig. 2. Inhibition of FGF- and VEGF-induced angiogenesis *in vivo*. (**A**) Shown are representative slit-lamp photographs of Swiss Webster mice corneas on day 5 post-implantation. Implanted pellets contained either bFGF or VEGF, and mice were treated with PBS (control) or PD 173074. An arrowhead marks the location of the implanted pellet. (**B**) Pellets containing bFGF or VEGF implanted in untreated mice produced a mean area of neovascularization of 5.9 mm^2 or 1.9 mm^2, respectively. PD 173074 given intraperitoneally at a dose of 1 mg/kg per day starting 3 days prior to pellet implantation inhibited bFGF-induced neovascularization by 86% ($P < 0.0001$) (black bars), and at a dose of 2 mg/kg per day inhibited VEGF-induced neovascularization by 81% ($P < 0.0001$) (gray bars). Error bars indicate the standard error of the mean.

autophosphorylation of FGFR1 in cultured cells. NIH 3T3 cells which express FGFR1 endogenously were treated with PD 173074 at various concentrations and then stimulated with aFGF and heparin. FGFR1 was immunoprecipitated from cell lysates, subjected to SDS–PAGE, and immunoblotted with antibodies to phosphotyrosine. PD 173074 inhibited autophosphorylation of FGFR1 in a dose-dependent manner with an IC_{50} in the range 1–5 nM (Figure 1B). Thus, both in *in vitro* assays and in cultured cells, PD 173074 is a potent inhibitor of FGFR1 kinase activity.

Because of the importance of the VEGF signaling pathway in angiogenesis, PD 173074 was tested as an inhibitor of VEGF receptor kinase activity in cultured cells. NIH 3T3 cells overexpressing VEGFR2 (Flk-1) (Millauer *et al.*, 1993) were treated with various concentrations of PD 173074 and stimulated with VEGF. Cell lysates were subjected to SDS–PAGE and immunoblotted with antibodies to phosphotyrosine. PD 173074 inhibited autophosphorylation of VEGFR2 with an IC_{50} of 100–200 nM (Figure 1C).

Inhibition of angiogenesis in vivo

Given the high potency and selectivity of PD 173074 for FGFR1 and VEGFR2, this compound was tested for its

Table II. Data collection and refinement statistics

Data collection					
Resolution (Å)	Observations (N)	Completeness (%)	Redundancy	R_{sym}[a] (%)	Signal $\langle I > \sigma I \rangle$
30.0–2.5	93535	94.5 (95.5)[b]	3.7	4.7 (25.2)[b]	12.4
Refinement[c]					
Resolution (Å)	Reflections (N)	*R*-value[d] (%)	Root-mean-square deviations		
			Bonds (Å)	Angles (°)	B-factors[e] ($Å^2$)
6.0 – 2.5	20340	20.4 (26.4)[f]	0.009	1.4	2.1

[a] $R_{sym} = 100 \times \Sigma_{hkl} \Sigma_i |I_i(hkl) - \langle I(hkl) \rangle| / \Sigma_{hkl} \Sigma_i I_i(hkl)$. Data are from one crystal.
[b] Value in parentheses is for the highest resolution shell.
[c] Atomic model includes 550 residues (two kinase molecules), two PD 173074 molecules and 191 water molecules (4573 atoms).
[d] *R*-value $= 100 \times \Sigma_{hkl} ||F_o(hkl)| - |F_c(hkl)|| / \Sigma_{hkl} |F_o(hkl)|$, where F_o and F_c are the observed and calculated structure factors, respectively ($F_o > 2\sigma$).
[e] For bonded protein atoms.
[f] Value in parentheses is the free *R*-value determined from 5% of the data.

ability to block angiogenesis *in vivo*. The model system chosen to study the *in vivo* effects of PD 173074 was the mouse cornea. In this angiogenesis model, a polymeric pellet embedded with an angiogenic factor such as bFGF is surgically implanted in the avascular mouse cornea near the temporal limbus (Kenyon *et al.*, 1996). After several days, a reproducible, non-inflammatory angiogenic response is readily observed.

Implantation of a pellet containing 100 ng of bFGF in the cornea of a Swiss Webster mouse stimulated extensive blood vessel formation originating from the temporal limbus (Figure 2A). Mice treated daily with PD 173074 by intraperitoneal injection exhibited dose-dependent inhibition of FGF-induced neovascularization. At the highest dose tested, 1 mg/kg per day, substantial inhibition of angiogenesis was observed, and in many cases complete suppression of the angiogenic response resulted (Figure 2A). There were no toxic effects observed in the mice at this dose.

The efficacy of PD 173074 as an inhibitor of VEGF-stimulated angiogenesis was tested in the same assay. VEGF at a dose of 200 ng provided a strong angiogenic stimulus in non-treated animals, albeit less so than bFGF (Figure 2B) as previously recognized (Kenyon *et al.*, 1996). PD 173074 administered daily at a dose of 2 mg/kg significantly reduced VEGF-induced angiogenesis, but was somewhat less effective in blocking VEGF-induced than FGF-induced angiogenesis.

Structure of PD 173074–FGFR1K

Crystal structures of the unphosphorylated (pre-activated) tyrosine kinase domain of FGFR1 (FGFR1K) have been determined previously in the absence and presence of a non-hydrolyzable ATP analog (AMP-PCP) (Mohammadi *et al.*, 1996a). For crystallographic studies of the PD 173074–FGFR1K complex, crystals of unphosphorylated FGFR1K were soaked in a solution containing PD 173074. The structure of the complex was refined at 2.5 Å resolution with a crystallographic *R*-value of 20% (6.0–2.5 Å data $>2\sigma$, *R*-free = 26%). Data collection and refinement statistics are given in Table II. The electron density map (Figure 3) shows good supporting density for the pyrido[2,3-*d*]pyrimidine ring system, the dimethoxy phenyl group (6-position) and the urea and *tert*-butyl groups (7-position), but shows weaker density for the butyl and diethylamino groups (2-position). These latter groups make only a modest contribution to potency but enhance aqueous solubility (Hamby *et al.*, 1997). Except where noted, comparable interactions between PD 173074 and FGFR1K are observed in the two complexes of the asymmetric unit.

PD 173074 binds in the ATP-binding cleft of FGFR1K, which lies between the two lobes of the kinase (Figure 4A). The pyrido[2,3-*d*]pyrimidine ring system occupies the same position as the ATP adenine (Figure 4B). Hydrophobic residues that line the pyrido[2,3-*d*]pyrimidine/adenine pocket include Leu484, Ala512, Tyr563, Ala564 and Leu630 (Figures 4A and 5). PD 173074 makes two hydrogen bonds with main-chain atoms of FGFR1K in the segment that connects the two kinase lobes (Figure 4B). N-3 of the pyrimidine ring is hydrogen-bonded to the amide nitrogen of Ala564, and the nitrogen of the butylamino group is hydrogen-bonded to the carbonyl oxygen of Ala564. The ATP adenine also makes two hydrogen bonds with main-chain atoms in this segment: one with the amide nitrogen of Ala564 via N-1 (in common with PD 173074), and the other with the carbonyl oxygen of Glu562 via N-6.

A third hydrogen bond is made between one of the dimethoxy groups of PD 173074 and the amide nitrogen of Asp641 (Figure 4A), a residue which is part of the protein kinase-conserved Asp-Phe-Gly triad at the beginning of the activation loop. The urea group attached to the pyrido[2,3-*d*]pyrimidine at the 7-position makes an internal hydrogen bond with N-8 of the ring system and is also hydrogen-bonded to a water molecule (Figure 5). This water molecule in turn is hydrogen-bonded to the side chains of protein kinase-conserved Lys514 and Asp641, which participate in MgATP coordination (reviewed in Taylor and Radzio-Andzelm, 1994). Curiously, this water molecule is well ordered in only one of the two PD 173074–FGFR1K complexes.

Compared with the unliganded FGFR1K structure, conserved Lys514 is the only residue that shows significant movement upon PD 173074 binding. The side chain of Lys514 adopts an alternative conformation which allows the dimethoxy phenyl substituent of the compound access to the back of the ATP-binding cleft, which is unoccupied in the structure of the complex of AMP-PCP with FGFR1K (Mohammadi *et al.*, 1996a) (Figure 6A and B). The plane of the phenyl ring is approximately perpendicular to the plane of the pyrido[2,3-*d*]pyrimidine rings, and van der

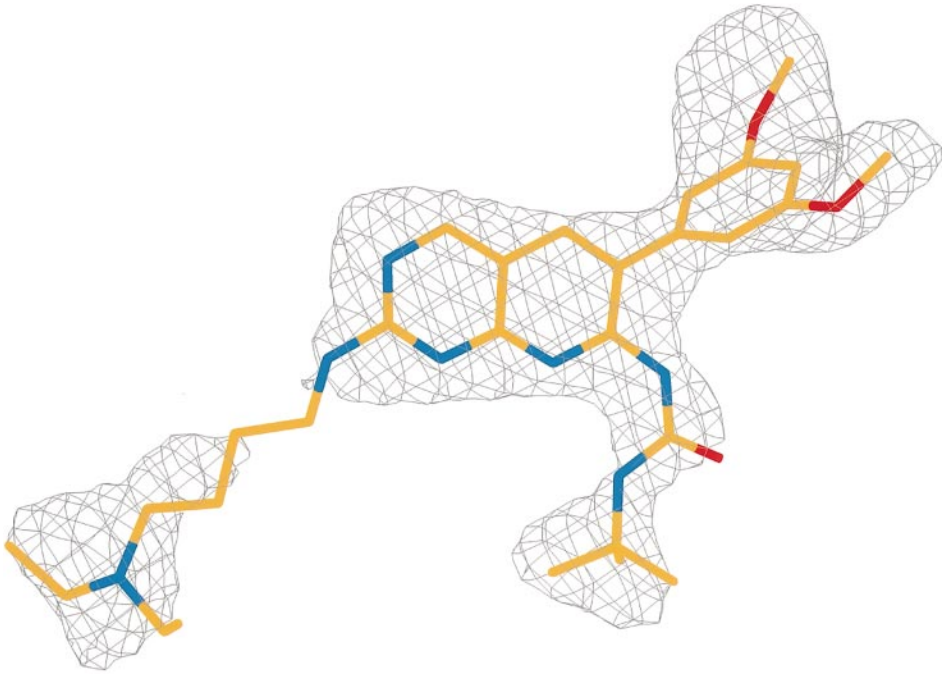

Fig. 3. Electron density map of PD 173074 bound to FGFR1K. F_o-F_c electron density map computed after simulated annealing (1000K) with PD 173074 omitted from the atomic model. The map was computed at 2.5 Å resolution and contoured at 2.5σ. Split-bond coloring is employed with carbon atoms orange, oxygen atoms red and nitrogen atoms blue. Prepared with SETOR (Evans, 1993).

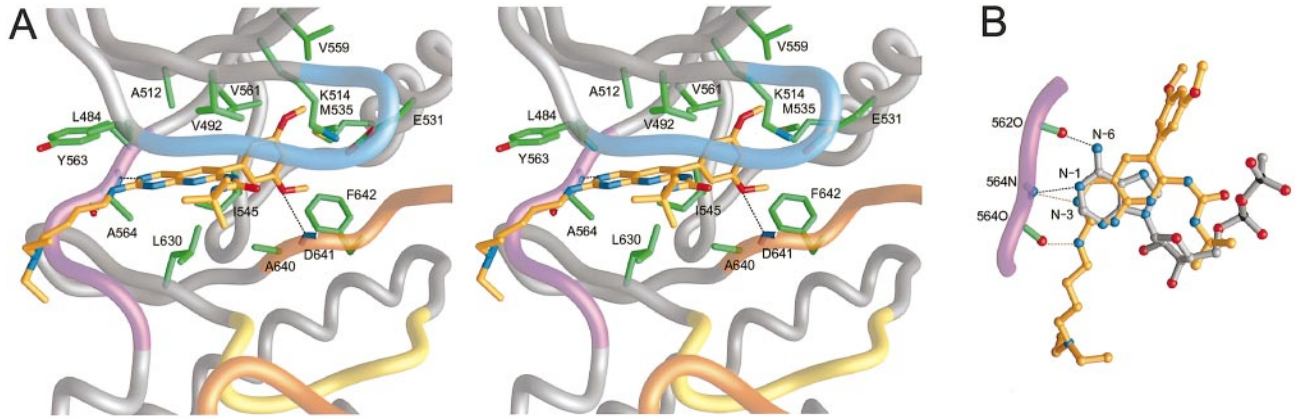

Fig. 4. Mode of PD 173074 binding to FGFR1K. (**A**) Stereo view of the PD 173074 binding pocket in FGFR1K. The side chains of residues that interact with the inhibitor are shown as well as main-chain atoms that participate in hydrogen bonding. Split-bond coloring is used with carbon atoms orange (PD 173074) or green (FGFR1K), oxygen atoms red, nitrogen atoms blue and sulfur atoms yellow. The FGFR1K main-chain representation is colored light blue for the nucleotide-binding loop, purple for the segment connecting the two kinase lobes, yellow for the catalytic loop and orange for the activation loop. Hydrogen bonds are shown as dashed lines. (**B**) Superposition of PD 173074 and AMP-PCP (Mohammadi *et al*., 1996a) bound to FGFR1K. View is approximately perpendicular to the pyrido[2,3-*d*]pyrimidine/adenine rings. Bonds and carbon atoms are colored orange (PD 173074), green (FGFR1K) or gray (AMP-PCP). Other atoms colored as in (A) with phosphorus atoms black. Hydrogen bonds are shown as black (AMP-PCP) or orange (PD 173074) dashed lines. Due to disorder, the γ phosphate of AMP-PCP is not modeled. Prepared with GRASP (Nicholls *et al.*, 1991).

Waals contacts are made between the dimethoxy phenyl group and the side chains of Lys514, Glu531, Met535, Ile545, Val559, Val561, Ala640 and Phe642 (Figures 4A and 5). As shown in Figure 6A, there is exceptional complementarity between PD 173074 and the surface of the ATP-binding cavity of FGFR1K. The total accessible surface area buried upon complexation of PD 173074 with FGFR1K is 1023 $Å^2$.

Determinants of selectivity

Structure–activity relationship (SAR) data indicate that binding affinity and selectivity for FGFR1 is attained through modification of the phenyl group attached to the 6-position of the pyrido[2,3-*d*]pyrimidine (Connolly *et al.*, 1997). Derivatization at the 6-position with just a phenyl ring yields a compound which shows weak selectivity for FGFR1 and has a 100-fold poorer IC_{50} than derivatization with a 3,5-dimethoxy phenyl. In general, derivatization at the 3- and 5-positions of the phenyl ring increase selectivity for FGFR1, especially when the attached group is larger than a methyl. The SAR data are in good agreement with the surface complementarity observed in the crystal structure of the complex (Figure 6A).

Although the Asp641-Phe-Gly triad at the beginning of

the activation loop is conserved in protein kinases, the conformation of this segment in the unphosphorylated form of protein kinases has been observed to differ (Hubbard *et al.*, 1994; Mohammadi *et al.*, 1996a; reviewed in Johnson *et al.*, 1996). Therefore, despite sequence conservation, the hydrogen bond to the main chain of Asp641 and the hydrophobic contacts with the side chains of Ala640 and Phe642 (Figures 4A and 5) are likely to contribute to the selectivity of PD 173074 for FGFR1. The C helix in the N-terminal lobe also shows positional heterogeneity among protein kinases (reviewed in Johnson *et al.*, 1996). The position of the C helix in FGFR1 is favorable for interaction with PD 173074; the side chains of Met535 and protein kinase-conserved Glu531 make van der Waals contacts with the dimethoxy phenyl substituent of PD 173074.

Table III shows the residues in FGFR1 that contact PD 173074, along with the corresponding residues in other protein kinases. Two key residues in determining selectivity appear to be Val559 and Val561. The side chains of these residues form part of the hydrophobic pocket in which the dimethoxy phenyl group of PD 173074 is situated. Most protein kinases have residues with larger side chains at one or both of these positions, especially serine/threonine kinases, and modeling studies predict that these residues would interfere sterically with the dimethoxy phenyl group (Trumpp-Kallmeyer *et al.*, 1998). Interestingly, both VEGFR1 and VEGFR2 have valine at the positions corresponding to Val559 and Val561 of FGFR1. Conservation of valine at these two positions is evidently why PD 173074 is an effective inhibitor of

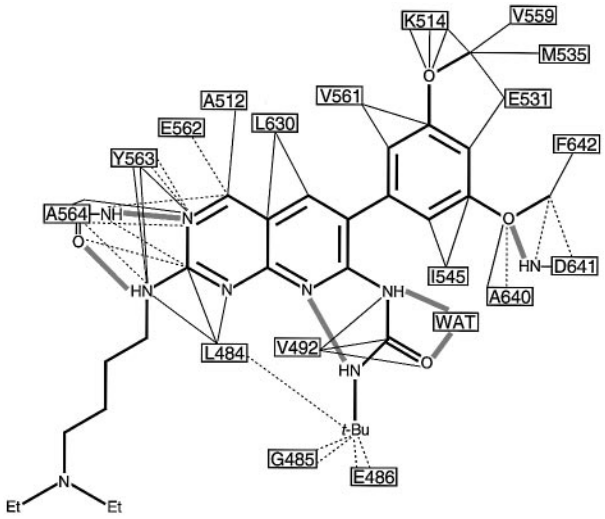

Fig. 5. Schematic diagram of interactions between FGFR1K and PD 173074. Shown are contacts for which the interatomic distance is ⩽3.8 Å. Thin solid lines denote contacts involving FGFR1K side-chain atoms, and thin dotted lines denote contacts involving FGFR1K main-chain atoms. Hydrogen bonds are shown as thick gray lines. No contacts are shown for the butyl and diethylamino groups due to the relative disorder of these atoms. Et = ethyl and *t*-Bu = *tert*-butyl.

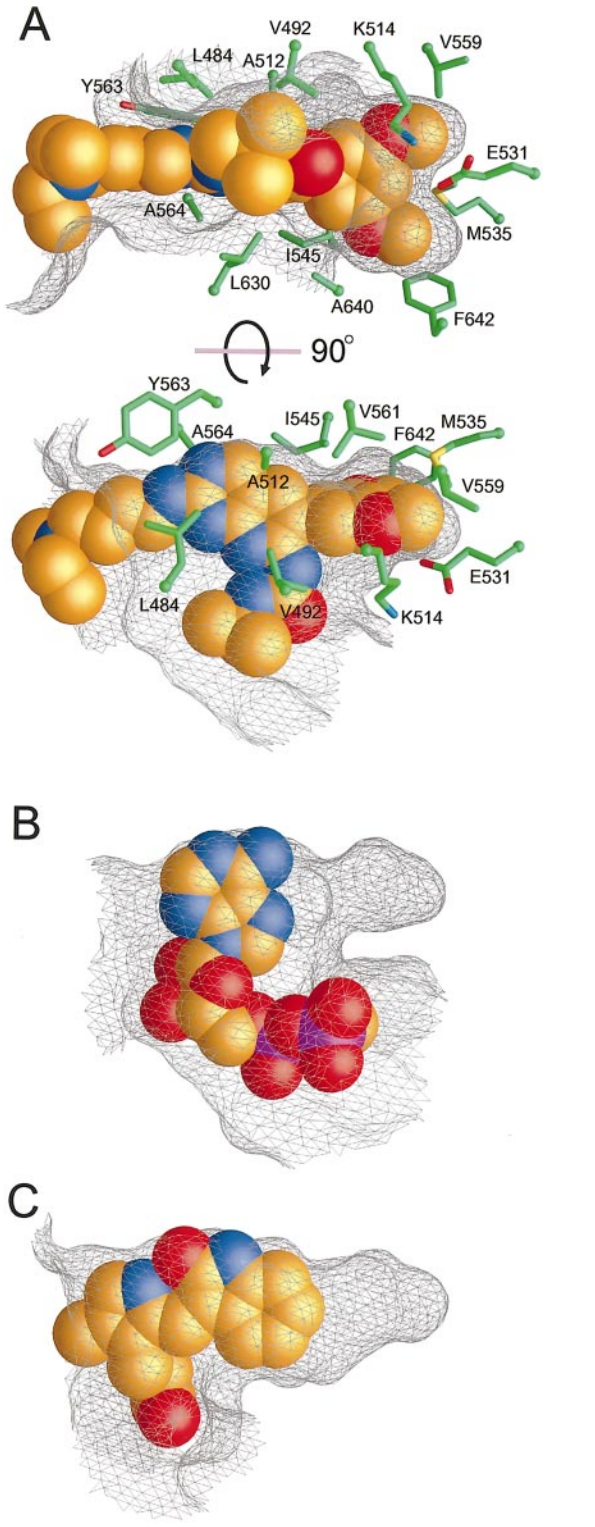

Fig. 6. Surface complementarity between PD 173074 and FGFR1K. (**A**) Shown in gray mesh representation is the surface of FGFR1K within 5 Å of PD 173074. The view in the top panel is approximately the same as in Figure 4A. The view in the bottom panel is 90° away as indicated, and is approximately the same as in Figure 3. Carbon atoms of PD 173074 are colored orange, oxygen atoms red and nitrogen atoms blue. Split-bond coloring is used for the side chains of FGFR1K that interact with PD 173074, with carbon atoms green, oxygen atoms red, nitrogen atoms blue and sulfur atoms yellow. The α-carbon position for each side chain is represented by a sphere. (**B**) Surface of FGFR1K in proximity to bound AMP-PCP (Mohammadi *et al.*, 1996a). The view is the same as in the bottom panel of (A). Same atom coloring as in (A) with phosphorus atoms colored purple. Due to disorder, the γ phosphate of AMP-PCP is not modeled. (**C**) Surface of FGFR1K in proximity to bound SU5402 (Mohammadi *et al.*, 1997). The view is the same as in the bottom panel of (A). Same atom coloring as in (A). Prepared with GRASP (Nicholls *et al.*, 1991).

Table III. Amino acid comparison in the ATP-binding cleft

FGFR1[a]	InsR	EGFR	PDGFRβ	VEGFR2	Src	MEK	PKCα
Leu484 (β1)[b]	●[c]	●	●	●	●	●	●
Val492 (β2)	●	●	●	●	●	●	●
Ala512 (β3)	●	●	●	●	●	●	●
Lys514 (β3)	●	●	●	●	●	●	●
Glu531 (αC)[d]	●	●	●	●	●	●	●
Met535 (αC)[d]	●	●	●	Leu	●	Leu	Leu
Ile545 (αC/β4)	Val	Cys	Val	Val	Val	Val	Thr
Val559 (β5)	●	Leu	Ile	●	Ile	Ile	Phe
Val561 (β5)	Met	Thr	Thr	●	Thr	Met	Met
Tyr563 (β5/αD)	Leu	Leu	●	Phe	●	His	●
Ala564 (β5/αD)	Met	Met	Cys	Ser	Met	Met	Val
Leu630 (β7)	Met	●	●	●	●	●	●
Ala640 (A-loop)[d]	Gly	Thr	Cys	Cys	●	Cys	●
Phe642 (A-loop)[d]	●	●	●	●	●	●	●

[a]Listed are residues of FGFR1 whose side chains interact (interatomic distance ⩽3.8 Å) with PD 173074.
[b]In parentheses is the secondary structural element in which the residue is located (Mohammadi *et al.*, 1996a). Two secondary structural elements separated by a slash implies the segment between the two elements.
[c]● = same residue as in FGFR1.
[d]Residues are in segments that show positional heterogeneity in protein kinases (see text).

VEGFR2 as well as of FGFR1. On this basis, one would predict that PD 173074 would not be a potent inhibitor of the Ang1 receptor TIE2, which contains leucine and isoleucine at these two positions.

We have determined previously the crystal structures of two oxindole-based compounds bound to FGFR1K (Mohammadi *et al.*, 1997). These ATP-competitive compounds are ~10^3 less potent than PD 173074 as inhibitors of FGFR1 autophosphorylation in NIH 3T3 cells. Although any differences in membrane permeability will contribute to this disparity, much of the potency difference is probably due to the extent to which the compounds engage FGFR1K residues. The total amount of accessible surface area buried in the SU5402-FGFR1K complex is 715 Å^2, versus 1023 Å^2 for PD 173074–FGFR1K. In particular, the portion of the ATP-binding cleft in which the dimethoxy phenyl group of PD 173074 binds is not utilized by the oxindole compounds (Figure 6A and C).

Conclusions

The pyrido[2,3-*d*]pyrimidine-based compound PD 173074 is a potent inhibitor of FGFR1, an effective inhibitor of VEGFR2 and a poor inhibitor of other protein kinases such as Src, the insulin and EGF receptors, and protein kinase C. Crystallographic analysis of the complex between PD 173074 and the tyrosine kinase domain of FGFR1 shows that there is exquisite surface complementarity between this compound and the ATP-binding cleft of FGFR1, which is evidently responsible for both the potency and selectivity of this compound. Although the ATP-binding cleft of protein kinases comprises hydrophobic residues that are reasonably well conserved, accumulating crystallographic and SAR data indicate that kinase selectivity can be achieved by small molecule inhibitors that exploit the numerous conservative substitutions present in this cleft. In a mouse corneal angiogenesis model, PD 173074 markedly suppressed neovascularization induced by bFGF or VEGF at a relatively low dose with no apparent toxicity. The selectivity characteristics of PD 173074 and its demonstrated ability to block angiogenesis *in vivo* make this an attractive lead compound in the pursuit of a therapeutic angiogenesis inhibitor.

Materials and methods

In vitro kinase inhibition assays

The *in vitro* kinase inhibition protocols have been described previously: FGFR1, PDGFRβ and Src (Panek *et al.*, 1997), EGFR (Fry *et al.*, 1997), insulin receptor (Fry *et al.*, 1994), PKC (Martiny-Baron *et al.*, 1993) and MEK (Dudley *et al.*, 1995). The ATP concentration was 5 μM in the assays for FGFR1, PDGFRβ, EGFR and Src, and 10 μM in the assays for the insulin receptor, PKC and MEK. Determination of K_i values was performed as described previously (Panek *et al.*, 1997).

Inhibition of FGFR1 and VEGFR2 autophosphorylation in NIH 3T3 cells

An NIH 3T3 cell line overexpressing VEGFR2 (Flk-1) has been described previously (Millauer *et al.*, 1993). This cell line also expresses FGFR1 endogenously. Cells (1×10^6) in DMEM supplemented with 10% calf serum were seeded in 10 cm^2 dishes and allowed to grow for 48 h. The medium was then removed and the cells were made quiescent in starvation medium (DMEM with 0.1% calf serum). After 18 h, the cells were incubated for 5 min with various concentrations of PD 173074 prepared in starvation medium. The cells were then stimulated with growth factor [VEGF (100 ng/ml) or aFGF (100 ng/ml) and heparin (10 μg/ml)] for 5 min at 37°C. The cells were washed with ice-cold PBS and lysed in 1 ml of lysis buffer (25 mM HEPES pH 7.5, 150 mM NaCl, 1% Triton X-100, 10% glycerol, 1 mM EGTA, 1.5 mM $MgCl_2$, 1 mM PMSF, 10 μg/ml aprotonin, 10 μg/ml leupeptin) containing phosphatase inhibitor (0.2 mM Na_3VO_4). For inhibition studies of FGFR1, cell lysates were immunoprecipitated with antibodies to FGFR1 (Mohammadi *et al.*, 1996b), and then analyzed by SDS–PAGE and immunoblotting with antibodies to phosphotyrosine. For inhibition studies of VEGFR2, cell lysates (20 μl) were analyzed directly by SDS–PAGE and immunoblotted with antibodies to phosphotyrosine.

Corneal neovascularization assay

Pellets were made from the slow release polymer Hydron (polyhydroxyethylmethacrylate) (Interferon Sciences, New Brunswick, NJ) and contain sucralfate (Bukh Meditiec, Valerose, Denmark) as a stabilizer as described (Kenyon *et al.*, 1996). Using aseptic technique, an intrastromal keratotomy was performed on Swiss Webster mice cornea. The mice were anesthetized with Metefane (methoxyflurane). The mouse eye was topically anesthetized with 0.5% proparacrine ophthalmic ointment (Henry Schein Inc., Melville, NY) and proptosed using forceps. With the aid of a dissecting microscope, a superficial vertical incision was made in the mouse cornea with a Microknife (Bristol-Myers Squibb Co., Jacksonville, FL). Using a von Graefe cataract knife (Miltex, Needham

Heights, MA) the superficial layer of the cornea was lifted and a micropocket was created for the insertion of the pellet. Smooth fine forceps (Sigma Chemical Co., St Louis, MO) were used to guide the pellet into the pocket, which was placed 0.5 or 1 mm from the limbic vascular plexus for VEGF or bFGF pellets, respectively. Erythromycin ophthalmic ointment was applied to prevent infection. Pellets contained either 100 ng bFGF, 200 ng VEGF or neither. PD 173074 was prepared in sterile fashion and administered intraperitoneally starting 3 days prior to or on the day of pellet implantation and then daily until day 5 post-implantation, whereupon slit-lamp photomicroscopy was performed. Mice were examined for infection or illness and weighed daily. The maximal vessel length extending from the limbic vessel to the pellet was measured and a circumferential zone of neovascularization was estimated as clock hours. An area of neovascularization was calculated in mm^2 as described (Klauber *et al.*, 1997). The mean, standard error of the mean and *P* values were determined using StatView 4.5 (Abacus Concepts).

X-ray data collection and structure refinement

Expression, purification and crystallization of FGFR1K were performed as described (Mohammadi *et al.*, 1996a). Crystals of unliganded FGFR1K grow in space group C2 with two molecules in the asymmetric unit and unit cell parameters when frozen of a = 208.8 Å, b = 57.4 Å, c = 66.2 Å and β = 107.6°. Crystals were soaked in 500 µl of stabilizing solution [25% polyethylene glycol 10000, 0.3 M $(NH_4)_2SO_4$, 0.1 M bis-Tris pH 6.5, 5% ethylene glycol] containing 2 mM PD 173074 at 4°C for 6 days. Data were collected on a Rigaku RU-200 rotating anode (Cu Kα) operating at 50 kV and 100 mA, and equipped with double-focusing mirrors and an R-AXIS IIC image plate detector. Crystals were flash-cooled in a dry nitrogen stream at –175°C. Data were processed using DENZO and SCALEPACK (Otwinowski, 1993). Difference Fourier electron density maps were computed using phases calculated from the structure of unliganded FGFR1K (Mohammadi *et al.*, 1996a). X-PLOR (Brünger, 1992) was used for simulated annealing and positional/B-factor refinement, and TOM/FRODO (Jones, 1985) was used for model building. The average B-factor is 45.9 $Å^2$ for all atoms, 46.0 $Å^2$ for FGFR1K atoms and 40.5 $Å^2$ for PD 173074 atoms.

Crystallographic coordinates

Crystallographic coordinates have been deposited in the Brookhaven Protein Data Bank, accession code 2FGI, with a 1 year hold.

Acknowledgements

We thank D.Fry, A.Kraker and D.Dudley for kinase assays and S.Trumpp-Kallmeyer for helpful discussions. S.R.H. is a recipient of a Kimmel Scholar Award from the Sidney Kimmel Foundation for Cancer Research. Equipment in the structural biology program at the Skirball Institute is partially supported by a grant from the Kresge Foundation. Requests for PD 173074 may be sent to pd_oncology@aa.wl.com.

References

Brünger,A.T. (1992) X-PLOR (Version 3.1) Manual. The Howard Hughes Medical Institute and Department of Molecular Biophysics and Biochemistry, Yale University, New Haven, CT, USA.

Carmeliet,P. *et al.* (1996) Abnormal blood vessel development and lethality in embryos lacking a single VEGF allele. *Nature*, **380**, 435–439.

Connolly,C.J.C. *et al.* (1997) Discovery and structure-activity studies of a novel series of pyrido[2,3-*d*]pyrimidine tyrosine kinase inhibitors. *Bioorg. Medicinal Chem. Lett.*, **7**, 2415–2420.

Davis,S. *et al.* (1996) Isolation of angiopoietin-1, a ligand for the TIE2 receptor, by secretion-trap expression cloning. *Cell*, **87**, 1161–1169.

Dudley,D.T., Pang,L., Decker,S.J., Bridges,A.J. and Saltiel,A.R. (1995) A synthetic inhibitor of the mitogen-activated protein kinase cascade. *Proc. Natl Acad. Sci. USA*, **92**, 7686–7689.

Dumont,D.J., Yamaguchi,T.P., Conlon,R.A., Rossant,J. and Breitman, M.L. (1992) tek, a novel tyrosine kinase gene located on mouse chromosome 4, is expressed in endothelial cells and their presumptive precursors. *Oncogene*, **7**, 1471–1480.

Dumont,D.J., Gradwohl,G., Fong,G.H., Puri,M.C., Gertsenstein,M., Auerbach,A. and Breitman,M.L. (1994) Dominant-negative and targeted null mutations in the endothelial tyrosine kinase, tek, reveal a critical role in vasculogenesis in the embryo. *Genes Dev.*, **8**, 1897–1909.

Evans,S.V. (1993) SETOR: Hardware lighted three-dimensional solid model representations of macromolecules. *J. Mol. Graphics*, **11**, 134–138.

Folkman,J. and D'Amore,P.A. (1996) Blood vessel formation: what is its molecular basis? *Cell*, **87**, 1153–1155.

Fong,G.H., Rossant,J., Gertsenstein,M. and Breitman,M.L. (1995) Role of the Flt-1 receptor tyrosine kinase in regulating the assembly of vascular endothelium. *Nature*, **376**, 66–70.

Fry,D.W., Kraker,A.J., McMichael,A., Ambroso,L.A., Nelson,J.M., Leopold,W.R., Connors,R.W. and Bridges,A.J. (1994) A specific inhibitor of the epidermal growth factor receptor tyrosine kinase. *Science*, **265**, 1093–1095.

Fry,D.W., Nelson,J.M., Slintak,V., Keller,P.R., Rewcastle,G.W., Denny,W.A., Zhou,H. and Bridges,A.J. (1997) Biochemical and antiproliferative properties of 4-[ar (alk)ylamino]pyridopyrimidines, a new chemical class of potent and specific epidermal growth factor receptor tyrosine kinase inhibitor. *Biochem. Pharmacol.*, **54**, 877–887.

Fujimoto,K., Ichimori,Y., Kakizoe,T., Okajima,E., Sakamoto,H., Sugimura,T. and Terada,M. (1991) Increased serum levels of basic fibroblast growth factor in patients with renal cell carcinoma. *Biochem. Biophys. Res. Commun.*, **180**, 386–392.

Hamby,J.M. *et al*. (1997) Structure-activity relationships for a novel series of pyrido[2,3-*d*]pyrimidine tyrosine kinase inhibitors. *J. Med. Chem.*, **40**, 2296–2303.

Hanahan,D. and Folkman,J. (1996) Patterns and emerging mechanisms of the angiogenic switch during tumorigenesis. *Cell*, **86**, 353–364.

Hubbard,S.R., Wei,L., Ellis,L. and Hendrickson,W.A. (1994) Crystal structure of the tyrosine kinase domain of the human insulin receptor. *Nature*, **372**, 746–754.

Jaye,M., Schlessinger,J. and Dionne,C.A. (1992) Fibroblast growth factor receptor tyrosine kinases: molecular analysis and signal transduction. *Biochem. Biophys. Acta*, **1135**, 185–199.

Johnson,L.N., Noble,M.E.M. and Owen,D.J. (1996) Active and inactive protein kinases: structural basis for regulation. *Cell*, **85**, 149–158.

Jones,T.A. (1985) Diffraction methods for biological macromolecules. Interactive computer graphics: FRODO. *Methods Enzymol.*, **115**, 157–171.

Kenyon,B.M., Voest,E.E., Chen,C.C., Flynn,E., Folkman,J. and D'Amato,R.J. (1996) A model of angiogenesis in the mouse cornea. *Invest. Ophthalmol. Vis. Sci.*, **37**, 1625–1632.

Kim,K.J., Li,B., Winer,J., Armanini,M., Gillett,N., Phillips,H.S. and Ferrara,N. (1993) Inhibition of vascular endothelial growth factor-induced angiogenesis suppresses tumour growth *in vivo*. *Nature*, **362**, 841–844.

Klauber,N., Parangi,S., Flynn,E., Hamel,E. and D'Amato,R.J. (1997) Inhibition of angiogenesis and breast cancer in mice by the microtubule inhibitors 2-methoxyestradiol and taxol. *Cancer Res.*, **57**, 81–86.

Libermann,T.A., Friesel,R., Jaye,M., Lyall,R.M., Westermark,B., Drohan,W., Schmidt,A., Maciag,T. and Schlessinger,J. (1987) An angiogenic growth factor is expressed in human glioma cells. *EMBO J.*, **6**, 1627–1632.

Martiny-Baron,G., Kazanietz,M.G., Mischak,H., Blumberg,P.M., Kochs,G., Hug,H., Marme,D. and Schachtele,C. (1993) Selective inhibition of protein kinase C isozymes by the indolocarbazole Go 6976. *J. Biol. Chem.*, **268**, 9194–9197.

Millauer,B., Wizigmann-Voos,S., Schnurch,H., Martinez,R., Moller,N.P., Risau,W. and Ullrich,A. (1993) High affinity VEGF binding and developmental expression suggest Flk-1 as a major regulator of vasculogenesis and angiogenesis. *Cell*, **72**, 835–846.

Millauer,B., Shawver,L.K., Plate,K.H., Risau,W. and Ullrich,A. (1994) Glioblastoma growth inhibited *in vivo* by a dominant-negative Flk-1 mutant. *Nature*, **367**, 576–579.

Mohammadi,M., Schlessinger,J. and Hubbard,S.R. (1996a) Structure of the FGF receptor tyrosine kinase domain reveals a novel autoinhibitory mechanism. *Cell*, **86**, 577–587.

Mohammadi,M., Dikic,I., Sorokin,A., Burgess,W.H., Jaye,M. and Schlessinger,J. (1996b) Identification of six novel autophosphorylation sites on fibroblast growth factor receptor 1 and elucidation of their importance in receptor activation snd signal transduction. *Mol. Cell. Biol.*, **16**, 977–989.

Mohammadi,M., McMahon,G., Sun,L., Tang,C., Hirth,P., Yeh,B.K., Hubbard,S.R. and Schlessinger,J. (1997) Structures of the tyrosine kinase domain of fibroblast growth factor receptor in complex with inhibitors. *Science*, **276**, 955–960.

Mustonen,T. and Alitalo,K. (1995) Endothelial receptor tyrosine kinases involved in angiogenesis. *J. Cell Biol.*, **129**, 895–898.

Nguyen,M., Watanabe,H., Budson,A.E., Richie,J.P., Hayes,D.F. and Folkman,J. (1994) Elevated levels of an angiogenic peptide, basic fibroblast growth factor, in the urine of patients with a wide spectrum of cancers. *J. Natl Cancer Inst.*, **86**, 356–361.

Nicholls,A., Sharp,K.A. and Honig,B. (1991) Protein folding and association: insights from the interfacial and thermodynamic properties of hydrocarbons. *Proteins*, **11**, 281–296.

Otwinowski,Z. (1993) Oscillation data reduction program. In L. Sawyer,L., Isaacs,N. and Burley,S. (eds) *Proceedings of the CCP4 Study Weekend*. SERC Daresbury Laboratory, Daresbury, United Kingdom, pp. 56–62.

Panek,R.L., Lu,G.H., Klutchko,S.R., Batley,B.L., Dahring,T.K., Hamby,J.M., Hallak,H., Doherty,A.M. and Keiser,J.A. (1997) *In vitro* pharmacological characterization of PD 166285, a new nanomolar potent and broadly active protein tyrosine kinase inhibitor. *J. Pharmacol. Exp. Ther.*, **283**, 1433–1444.

Partanen,J., Armstrong,E., Makela,T.P., Korhonen,J., Sandberg,M., Renkonen,R., Knuutila,S., Huebner,K. and Alitalo,K. (1992) A novel endothelial cell surface receptor tyrosine kinase with extracellular epidermal growth factor homology domains. *Mol. Cell. Biol.*, **12**, 1698–1707.

Puri,M.C., Rossant,J., Alitalo,K., Bernstein,A. and Partanen,J. (1995) The receptor tyrosine kinase TIE is required for integrity and survival of vascular endothelial cells. *EMBO J.*, **14**, 5884–5891.

Relf,M. *et al*. (1997) Expression of the angiogenic factors vascular endothelial cell growth factor, acidic and basic fibroblast growth factor, tumor growth factor beta-1, platelet-derived endothelial cell growth factor, placenta growth factor and pleiotrophin in human primary breast cancer and its relation to angiogenesis. *Cancer Res.*, **57**, 963–969.

Risau,W. (1997) Mechanisms of angiogenesis. *Nature*, **386**, 671–674.

Sato,T.N., Tozawa,Y., Deutsch,U., Wolburg-Buchholz,K., Fujiwara,Y., Gendron-Maguire,M., Gridley,T., Wolburg,H., Risau,W., Qin,Y. (1995) Distinct roles of the receptor tyrosine kinases Tie-1 and Tie-2 in blood vessel formation. *Nature*, **376**, 70–74.

Shalaby,F., Rossant,J., Yamaguchi,T.P., Gertsenstein,M., Wu,X.F., Breitman,M.L. and Schuh,A.C. (1995) Failure of blood-island formation and vasculogenesis in Flk-1-deficient mice. *Nature*, **376**, 62–66.

Suri,C., Jones,P.F., Patan,S., Bartunkova,S., Maisonpierre,P.C., Davis,S., Sato,T.N. and Yancopoulos,G.D. (1996) Requisite role of angiopoietin-1, a ligand for the TIE2 receptor, during embryonic angiogenesis. *Cell*, **87**, 1171–1180.

Taylor,S.S. and Radzio-Andzelm,E. (1994) Three protein kinase structures define a common motif. *Structure*, **2**, 345–355.

Trumpp-Kallmeyer,S., Rubin,R.J., Humblet,C., Hamby,J.M. and Showalter,H.D.H. (1998) Development of a binding model to protein tyrosine kinases for substituted pyrido[2,3-*d*]pyrimidine inhibitors. *J. Med. Chem.*, **41**, 1752–1763.

Ullrich,A. and Schlessinger,J. (1990) Signal transduction by receptors with tyrosine kinase activity. *Cell*, **61**, 203–212.

Wang.,Y. and Becker,D. (1997) Antisense targeting of basic fibroblast growth factor and fibroblast growth factor receptor-1 in human melanomas blocks intratumoral angiogenesis and tumor growth. *Nature Medicine*, **8**, 887–893.

Yoshiji,H., Harris,S.R. and Thorgeirsson,U.P. (1997) Vascular endothelial growth factor is essential for initial but not continued *in vivo* growth of human breast carcinoma cells. *Cancer Res.*, **57**, 3924–3928.

Received July 2, 1998; revised July 20, 1998;
accepted August 14, 1998